Research Article

Journal of RAMAN SPECTROSCOPY

Received: 8 October 2010 Accepted: 20 January 2011 Published online in Wiley Online Library: 25 March 2011

(wileyonlinelibrary.com) DOI 10.1002/jrs.2922

Phase-shaping strategies for coherent anti-Stokes Raman scattering†

A. C. W. van Rhijn,* M. Jurna, A. Jafarpour, J. L. Herek and H. L. Offerhaus

The identification of large molecules in complex environments requires probing of multiple vibrational resonances rather than a single resonance. Phase-shaping the excitation pulses allows the coherent mixing of several resonances so that the presence of molecules can be inferred directly from the integrated output pulse energy. This avoids the need for the collection of spectra or multiple measurements. This article describes a particular implementation for coherent anti-Stokes Raman scattering microscopy that uses a broadband pump and probe field in combination with a narrowband Stokes field. We numerically study the possibilities of optimizing selectivity, specificity, and sensitivity by precalculating pulse shapes using an evolutionary algorithm.

Keywords: ultrafast nonlinear optics; coherent anti-Stokes Raman scattering; nonlinear microscopy; pulse shaping; evolutionary algorithms

Introduction

Coherent anti-Stokes Raman scattering (CARS) has been successfully used in spectroscopy and microscopy since the development of (tunable) pulsed laser sources.[1] Over the last years, there has been a surge of interest in CARS due to the availability of new sources that allow video-rate imaging speeds and sensitivity levels that open up new applications.[2] In CARS, molecular vibrations are excited coherently by a combination of a pump (ω_p) and Stokes (ω_s) pulse. Subsequently, a probe (ω_{pr}) pulse, which is often derived from the same pulse as the pump, generates the CARS signal ($\omega_c = \omega_p - \omega_s + \omega_{pr}$).

A molecule can be thought of as analogous to an ensemble of mass–spring systems with a number of resonant frequencies. Each of these frequencies yields a peak in the amplitude spectrum and a phase step in the phase profile. The phase changes from 0 to $-\pi$, for an isolated resonance, but when multiple frequencies overlap, these resonances combine to create a complicated overall phase response, such as the examples presented in Fig. 2(d–f).

As CARS is a coherent (parametric) process, the signal consists of the coherent addition of the response of all the molecules in the excitation volume. The measured CARS is also affected by a nonresonant background. This nonresonant response to which all molecules contribute can reach considerable strength and even dominate the resonant CARS spectrum. Much effort has been put into the separation of this nonresonant background from the resonant signal. The relative phase of this nonresonant response (with respect to the phase of the driving field at the vibrational wavenumber) is zero so that the response is purely real. The imaginary part of the complex CARS field does not contain this nonresonant component. Knowledge of, or control over, the phase of the CARS signal allows the suppression of the nonresonant component.[3]

Phase-shaped CARS

Although very successful, narrowband CARS[4] (Fig. 1(a)) has a hard time in distinguishing minority constituents in a complex background when a unique identifying spectral feature is lacking. Often in biological applications, the targets for imaging are large molecules in complex cellular environments. In such cases, several spectral features have to be monitored to assign the observed signal to particular constituents. Preferably, all these features are monitored simultaneously to ensure a correct comparison. Broadband excitation, where several resonances are covered simultaneously, achieves this goal.[5–7] Collecting spectra is a relatively time-consuming activity, however, and it was realized that customized (phase-shaped) broadband pulses can also be used to excite or probe selectively.[8–14] These phase-shaped pulses are sometimes referred to as 'molecular music', in that the phase modulation of frequencies is analogous to the specific arrangement of notes in a melody. The goal is to create an excitation field that the target molecules 'dance most passionately to'. In this case, the passion refers to the coherent addition of the motion of different vibrational modes so that a peak in the motion in the time domain is created that favors the nonlinear interaction with the probe. The nonresonant component can be rejected by making sure that, for a constant and real component, the response averages out to zero over the duration of the probe.

In single-pulse CARS, introduced by Silberberg *et al.*[15,16], ω_p, ω_s and ω_{pr} are all parts of the same broadband pulse. These experiments mainly employ broadband pump and Stokes pulses, in combination with a relatively narrow probe pulse. Power and resolution available to address vibrations are not constant over

* *Correspondence to: A. C. W. van Rhijn, MESA+ Institute for Nanotechnology, Faculty of Science and Technology (TNW), University of Twente, The Netherlands. E-mail: Alexander.vanrhijn@utwente.nl*

† *This article is part of the Journal of Raman Spectroscopy special issue entitled "Proceedings of the 9th European Conference on Nonlinear Optical Spectroscopy (ECONOS), Bremen, Germany, June 21–23, 2010" edited by Peter Radi, PSI, Villigen, Switzerland, and Arnulf Materny, Jacobs University, Bremen, Germany.*

Optical Sciences Group, MESA+ Institute for Nanotechnology, Faculty of Science and Technology (TNW), University of Twente, The Netherlands

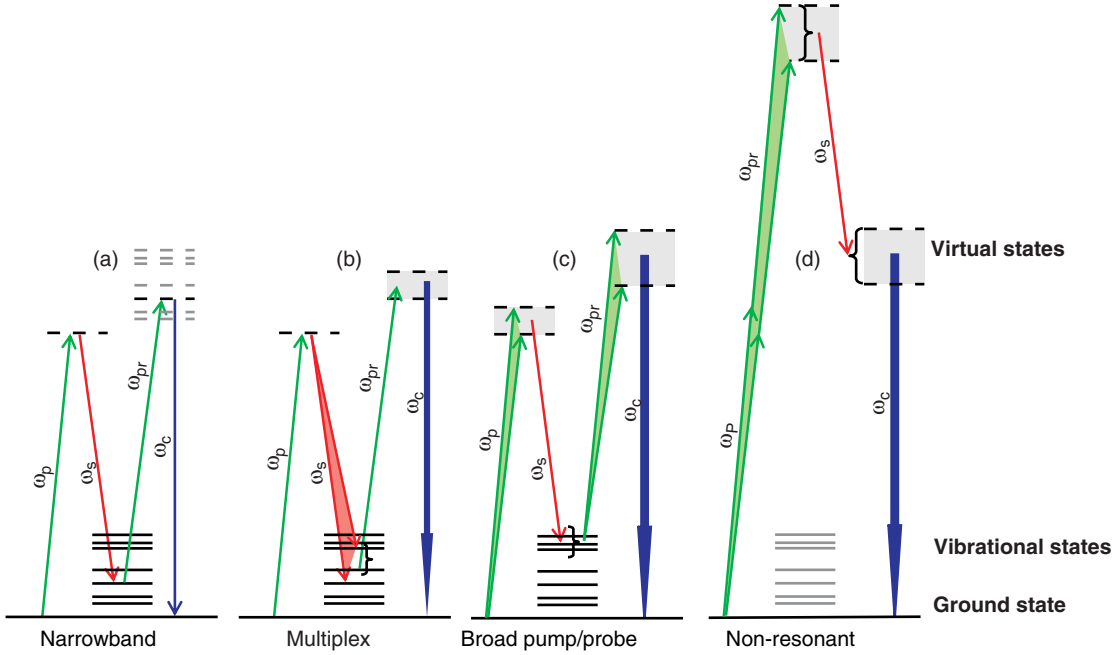

Figure 1. Energy level diagram for (a) narrowband CARS, (b) multiplex CARS, (c) broadband pump and probe CARS and (d) nonresonant four-wave mixing.

the bandwidth. For higher difference frequencies, the selectivity progressively degrades. We employ a broadband pump and probe pulse in combination with a narrowband Stokes pulse (Fig. 1(c)), providing a more constant resolution over the entire bandwidth.

Generally, the CARS process can be described by a convolution of the input fields and a multiplication with the molecular response:

$$I_{\mathrm{CARS}}(\omega) \propto |[(|E_{\mathrm{pump}}(\omega)|e^{i\Phi_{\mathrm{pump}}(\omega)} \otimes |E^{*}_{\mathrm{Stokes}}(\omega)|e^{-i\Phi_{\mathrm{Stokes}}(\omega)}) \cdot \chi^{(3)}(\omega)] \otimes |E_{\mathrm{probe}}(\omega)|e^{i\Phi_{\mathrm{probe}}(\omega)}|^2. \quad (1)$$

For a degenerate broadband pump and probe and narrowband Stokes pulse, this can be approximated as

$$I_{\mathrm{CARS}}(\omega) \propto |[|E(\omega+\omega_s)|e^{i\Phi(\omega+\omega_s)} \cdot \chi^{(3)}(\omega)] \otimes |E(\omega)|e^{i\Phi(\omega)}|^2. \quad (2)$$

The combination of a broadband pump pulse and a narrowband Stokes pulse excites multiple vibrations, where the spectral phase profile of the pump pulse is projected directly on the molecular response. By tuning the wavelength of the Stokes pulse, it is possible to access different vibrational regions. Due to the interaction with both a broadband pump and probe pulse, the resulting CARS signal is a broadband signal that contains nonresonant background and contributions from different pathways and interferences between vibrational resonances. The vibrational resonances are not directly apparent from the obtained CARS spectrum as in multiplex CARS[17–19] (Fig. 1(b)). Instead, we use spectral phase-shaping of the broadband pump and probe pulse to obtain vibrational information. The nonresonant background (Fig. 1(d)) is suppressed by taking a measurement with a phase profile and its inverse and subtracting them from each other. We previously reported on an intuitive phase-shaping strategy based on mimicking the inherent π-phase step of a resonance[20,21]. However, to fully exploit the interactions between the different excited vibrational resonances, a more complex phase profile is required. To calculate this profile, detailed knowledge of the vibrational phase response is required.

Obtaining the Vibrational Phase Response

The vibrational phase response can be directly measured using heterodyne detection[22] or vibrational phase contrast CARS.[23] Several other indirect techniques exist that retrieve the vibrational phase from a recorded broadband CARS spectrum.[24–27]

Here we introduce a method for determining the vibrational phase response based on spectral fitting with an evolutionary algorithm[28] of spontaneous Raman scattering data.[29] Spontaneous Raman spectra directly yield only the amplitude and wavenumber of vibrational resonances, but fitting the imaginary part of a sum of individual vibrational line shapes (Eqn 3) to the spontaneous Raman spectrum allows retrieval of the vibrational phase of the molecular response.

$$I_{\mathrm{Raman}}(\omega) \propto \Im[\chi^{(3)}(\omega)] = \Im\left[\chi^{(3)}_{\mathrm{NR}} + \sum_R \frac{A_R}{(\omega_R^2 - \omega^2 + 2i\omega\gamma_R)}\right] \quad (3)$$

We use a class of evolutionary algorithms, known as the evolution strategy, to solve the fitting problem by trying an initial spectral amplitude and phase profile and successive iterations. The employed evolution strategy uses the covariance matrix of parameters to continuously rotate and adapt the set of candidate solutions, and is referred to as covariance matrix adaptation evolution strategy (CMA-ES).[30] Details of the code implementing CMA-ES are reported elsewhere.[31] Spontaneous Raman scattering is free from nonresonant background, so the nonresonant part of the molecular response, $\chi^{(3)}_{\mathrm{NR}}$, cannot be directly inferred from the fit and has to be estimated. The nonresonant background can be added either as a constant value or as an arbitrary function of wavenumber. The spontaneous Raman scattering spectra and the associated fits for poly(methyl methacrylate)(PMMA), polystyrene and polyethene are shown in Fig. 2(a–c). The corresponding phases are shown in Fig. 2(d–f).

Journal of RAMAN SPECTROSCOPY

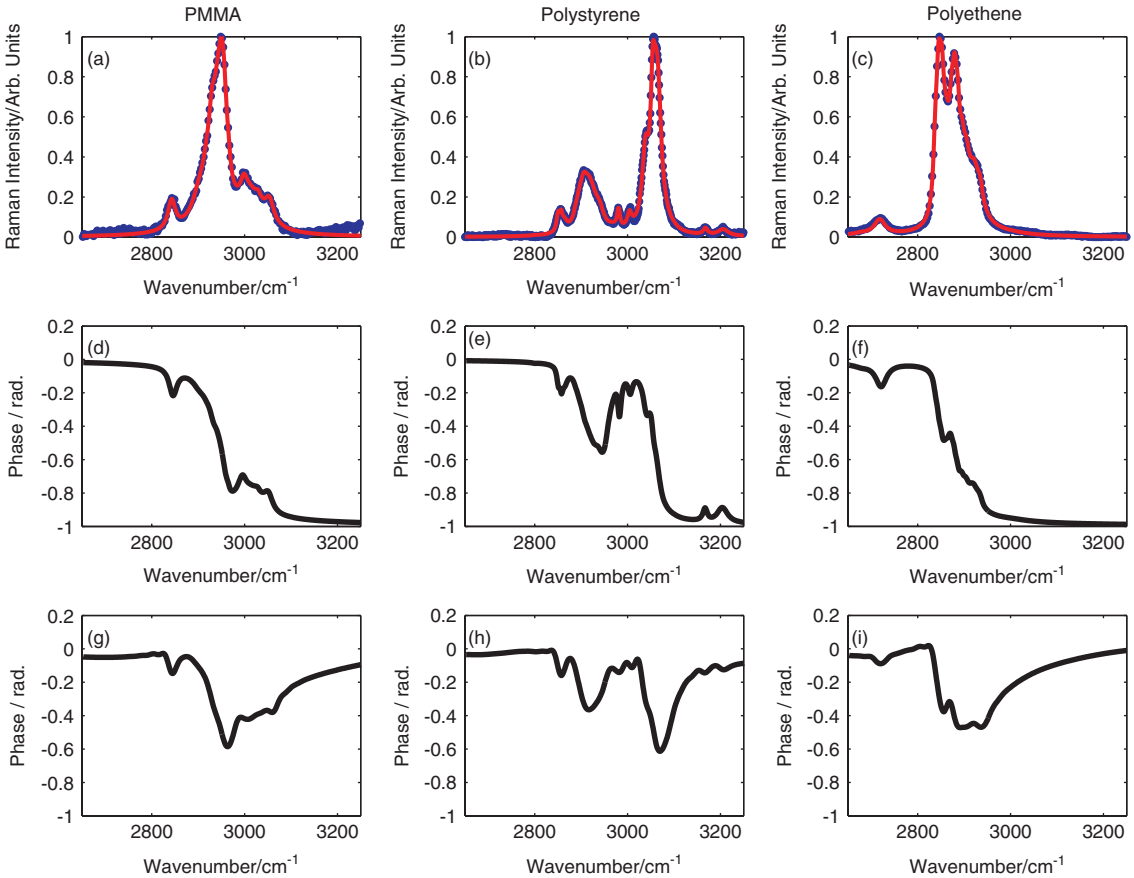

Figure 2. Spontaneous Raman spectrum (blue) and fit (red) of (a) PMMA, (b) polystyrene (c) polyethene and (d–f) the associated vibrational phases. The bottom row shows the optimal excitation phase for maximum CARS signal for (g) PMMA, (h) polystyrene, and (i) polyethene.

Pulse Optimization

Using the vibrational phase information of the molecule, the molecular response, $\chi^{(3)}(\omega)$, can be constructed. This molecular response is used to numerically calculate the CARS signal that input pulses with certain phase profiles generate (Eqn 2). Our goal is optimize the CARS signal of a specific molecule from a given set of molecules. We employ CMA-ES to find a spectral phase profile $\Phi_{opt}(\omega)$ that maximizes the difference in integrated CARS signal, integrated over the full bandwidth of the pulse, between a pump and probe pulse with a spectral phase $\Phi_{opt}(\omega)$ and a pump and probe pulse with (the inverse) spectral phase $-\Phi_{opt}(\omega)$. As mentioned before, this difference signal is free from purely nonresonant background. However, it is not free from mixing between the resonant signal and the non-resonant background.

The pump (= probe) pulse is assumed to have a Gaussian spectral power distribution with a center wavenumber of 12 400 cm^{-1} (806.5 nm) and a full width at half-maximum (FWHM) of 400 cm^{-1} (26 nm). The Stokes pulse is assumed to have a wavenumber of 9395.85 cm^{-1} (1064.3 nm) and an infinitesimally small bandwidth. For these simulations, the spectral phase profile is optimized by the CMA-ES on 80 points, divided evenly over 1021 cm^{-1}. This phase profile is extended to 4096 points by cubic spline interpolation in order to improve the resolution when calculating the CARS response. The CMA algorithm uses 20 parents and a population size of 40 per generation. The nonresonant background is assumed to be constant with a ratio between resonant and nonresonant response of 5 : 1 (peak to baseline). Optimizations with different ratios of nonresonant background showed similar results, as the purely nonresonant signal is discarded by looking at the difference CARS signal. The mixing between resonant and nonresonant signal influences the depth of the phase jumps in the optimized phase, but the general shape remains the same.

The obtained excitation phase profiles for maximum CARS signal for PMMA, polystyrene and polyethene are shown in Fig. 2(g–i) and mainly follow the general shape of the molecular phase response. At high wavenumbers, the phase returns to 0 instead of $-\pi$ due to the mixing between the resonant signal and the nonresonant background. The obtained CARS difference signal is about an order of magnitude more intense than the CARS signal from a 15-ps (1 cm^{-1}) pump and probe pulse, with the same pulse energy, focused on the main resonance of polystyrene. This comparison is based on a pure substance, with a constant nonresonant background of 20% (peak to baseline).

Even though the optimization of the CARS signal from a single component is useful, the true power of applying complex phase shapes is in optimizing the signal from a component while suppressing the signal from other components. In this study, we look at a combination of PMMA, polystyrene and polyethene, which have several overlapping resonances in the 3000 cm^{-1} region.

Using CMA-ES optimization, we are able to find spectral phase profiles that maximize the CARS signal for either of the three substances while simultaneously reducing the contributions of the other two substances. Given precise enough control over the spectral phase, contrast ratios of 500 : 1 are obtainable. The amount of CARS difference signal for the selected component is about

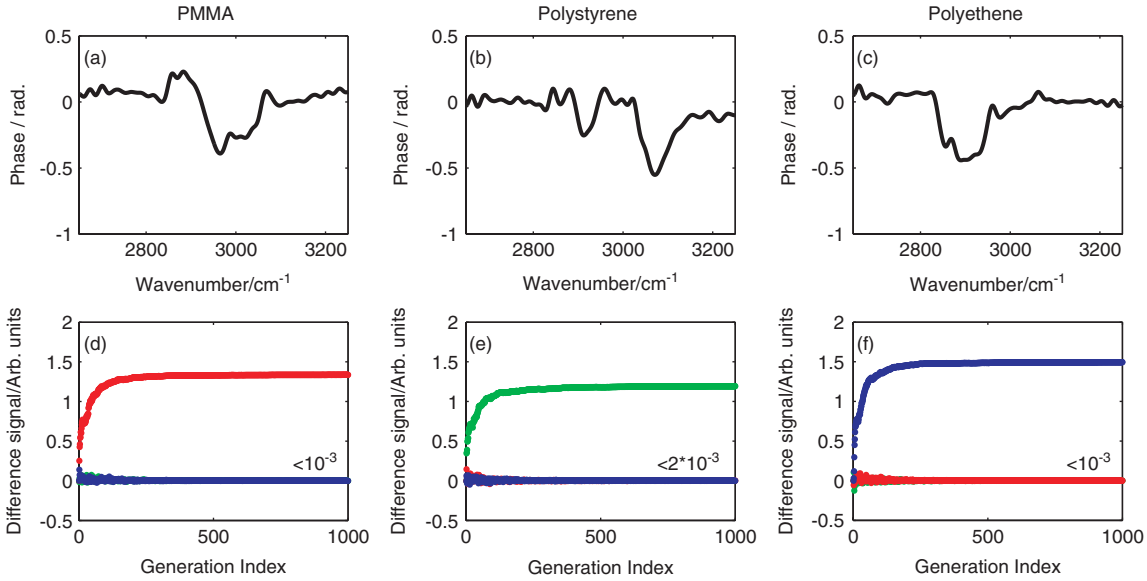

Figure 3. Selective excitation phases for (a) PMMA, (b) polystyrene and (c) polyethene and (d–f) the associated optimization curves, showing the obtained difference intensities for PMMA (red), polystyrene (green), and polyethene (blue).

90% of the signal obtained with the single substance optimization without suppression. This means that by suppressing the two other components, we only lose 10% of the signal of our component of interest. The resulting phase shapes and optimization curves are shown in Fig. 3. Note that the phase profiles no longer follow the general shape of the phase response of the molecule of interest (compare, e.g. Figures 2(g) and 3(a)).

Robustness of Optimal Profiles

In samples, there are often multiple components present simultaneously in the focal volume. Therefore, it is important not only to look at the response for a pure substance but also to consider the homodyne mixing of CARS fields from different substances within the focal volume. The resulting CARS signal for different mixtures of PMMA, polystyrene and polyethene within the focal volume is shown in Fig. 4(a–c) in the form of a ternary plot. Each of these three subfigures shows the results for the optimal phase profile that selectively excites PMMA, polystyrene or polyethene, respectively.

It can be seen that there is a close-to-linear dependence between the obtained CARS difference signal and the concentration for most mixtures, except near the region where there is less than a few percent of the substance that was optimized present in the focal volume compared to the suppressed substances. For the optimized profiles for PMMA and polystyrene, there is a band of mixing combinations, where the signal from small amounts of the substance of interest is suppressed due to mixing with the signal of the suppressed substances (Fig. 4(d–h). In effect, this will limit the obtainable contrast ratio to about 25 : 1. Furthermore, mixing between the signals from both suppressed components can produce a stronger signal than both components would produce by themselves. It can be seen in Fig. 4(e and f) that, in the case of the PMMA- or polystyrene-optimized profiles, mixing between the two suppressed components generates a negative difference signal, which can be easily distinguished from the positive difference signal that the component of interest generates. In the case of the polyethene optimized profile (Fig. 4(g)), there is a positive difference signal for mixing between PMMA and polystyrene however, which will limit selectivity. Optimization objectives that take these mixing terms into account could potentially solve this problem.

To get a better understanding of the required resolution of phase-shaping, we also investigate the effect of changing the number of parameters used to optimize the phase shape. In this case, we look at the optimization of selective excitation of PMMA for a varying number of parameters. It can be seen from Fig. 5 that the minimum amount of parameters required to accurately model the optimal phase function is about 40. A higher number does not significantly increase or decrease the amount of obtained signal or the contrast ratio. The number of elements on the phase shaper has to be higher, so that the applied phase function matches with the smooth interpolation between the parameters of the optimized phase function. Further improvements in terms of optimization and number of parameters can be obtained by tailoring the basis set of parameters that define the phase function.[32]

Conclusion

Tailored broadband pulses have the potential to revolutionize CARS by significantly improving the selectivity, specificity and sensitivity. We show the feasibility of using an evolutionary algorithm to obtain the complex vibrational phase response from spontaneous Raman scattering spectra and using this information to pre-optimize pulse shapes. We use a test case of a sample containing PMMA, polystyrene and polyethene and show a contrast ratio of 500 : 1 or better for each separate substance compared to the other two in the case of pure substances. In the case of mixing of the CARS fields due to multiple resonant substances in the focal volume, the obtained contrast ratio decreases to 25 : 1. The obtained phase shapes are characterized by 40 parameters over a 1021 cm^{-1} region, so that the required resolution for applying these phase shapes is limited and is within reach of current commercial shapers.

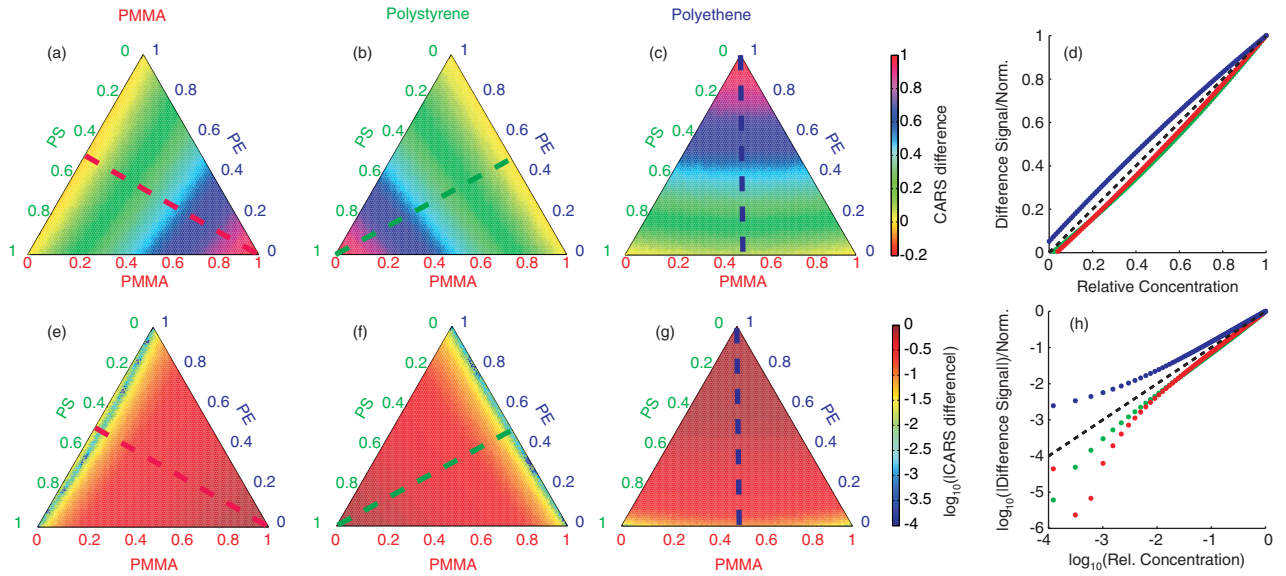

Figure 4. CARS difference signal for a mixture of different ratios of PMMA, polystyrene and polyethene in the focal volume for the selective excitation phase of (a) PMMA, (b) polystyrene and (c) polyethene. In (d), the signal dependence is shown along slices in the ternary plot, where the relative concentration of the optimized component (red for PMMA, green for polystyrene, blue for polyethene) goes from 1 to 0, with a 50%/50% ratio between the other resonant components. The dashed line indicates an ideal linear dependence. (e–g) The $\log_{10}$ of the absolute value of (a–c). (h) The dependence of the signal as in (d), but on a $\log_{10}/\log_{10}$ scale.

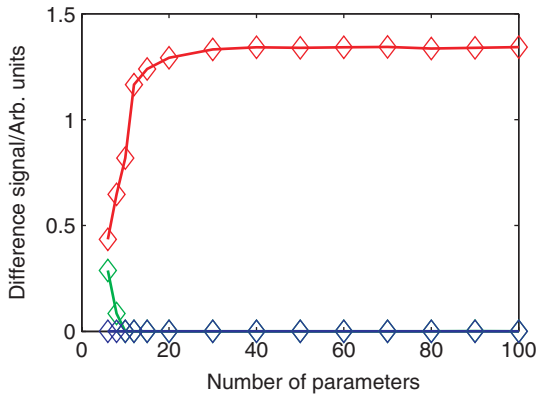

Figure 5. CARS difference signal for PMMA (red), polystyrene (green) and polyethene (blue) as a function of number of parameters that the pulse is optimized with for selective excitation of PMMA.

Acknowledgements

This research has been supported by the 'Stichting voor Fundamenteel Onderzoek der Materie' (FOM, Grant No. 03TF78-3), which is supported financially by Nederlandse Organisatie voor Wetenschappelijk Onderzoek (NWO). This work is also supported by the IOP (Innovatiegerichte Onderzoeksprogramma's) Photonic Devices program managed by the Technology Foundation STW (Stichting Technische Wetenschappen) and AgentschapNL.

References

[1] P. D. Maker, R. W. Terhune, *Phys. Rev. Lett.* **1965**, *137*, A801.
[2] J. Cheng, A. Volkmer, X. S. Xie, *J. Opt. Soc. Am. B* **2002**, *19*, 1363.
[3] E. O. Potma, C. L. Evans, X. S. Xie, *Opt. Lett.* **2006**, *31*, 241.
[4] C. L. Evans, X. S. Xie, *Annu. Rev. Anal. Chem.* **2008**, *1*, 883.
[5] J. X. Chen, A. Volkmer, L. D. Book, X. S. Xie, *J. Phys. Chem. B* **2002**, *106*, 8493.
[6] H. Kano, H. Hamaguchi, *Opt. Express* **2005**, *13*, 1322.
[7] G. W. H. Wurpel, J. M. Schins, M. Müller, *J. Phys. Chem. B* **2004**, *108*, 3400.
[8] D. Oron, N. Dudovich, Y. Silberberg, *Phys. Rev. Lett.* **2002**, *89*, 273001.
[9] D. Oron, N. Dudovich, Y. Silberberg, *Phys. Rev. A* **2004**, *70*, 023415.
[10] S. O. Konorov, X. G. Xu, J. W. Hepburn, V. Milner, *Phys. Rev. A* **2009**, *79*, 031801.
[11] V. V. Lozovoy, B. Xu, J. C. Shane, M. Dantus, *Phys. Rev. A* **2006**, *74*, 041805.
[12] J. Konradi, A. K. Singh, A. Materny, *Phys. Chem. Chem. Phys.* **2005**, *7*, 3574.
[13] J. Konradi, A. Scaria, V. Namboodiri, A. Materny, *J. Raman Spectrosc.* **2007**, *38*, 1006.
[14] S. D. McGrane, R. J. Scharff, M. Greenfield, D. S. Moore, *New J. Phys.* **2009**, *11*, 105047.
[15] N. Dudovich, D. Oron, Y. Silberberg, *Nature* **2002**, *418*, 512.
[16] D. Oron, N. Dudovich, Y. Silberberg, *Phys. Rev. Lett.* **2003**, *90*, 213902.
[17] A. Voroshilov, C. Otto, J. Greve, *Appl. Spectrosc.* **1996**, *50*, 78.
[18] H. Kano, H. Hamaguchi, *Appl. Phys. Lett.* **2005**, *86*, 121113.
[19] H. Rinia, M. Bonn, M. Müller, *J. Phys. Chem. B.* **2005**, *110*, 4472.
[20] S. Postma, A. C. W. van Rhijn, J. P. Korterik, P. Gross, J. L. Herek, H. L. Offerhaus, *Opt. Express* **2008**, *16*, 7985.
[21] A. C. W. van Rhijn, S. Postma, J. P. Korterik, J. L. Herek, H. L. Offerhaus, *J. Opt. Soc. Am. B.* **2009**, *26*, 559.
[22] M. Jurna, J. P. Korterik, C. Otto, J. L. Herek, H. L. Offerhaus, *Opt. Express* **2008**, *16*, 15863.
[23] M. Jurna, J. P. Korterik, C. Otto, J. L. Herek, H. L. Offerhaus, *Phys. Rev. Lett.* **2009**, *103*, 043905.
[24] S. H. Lim, A. G. Caster, O. Nicolet, S. R. Leone, *J. Phys. Chem. B* **2006**, *110*, 5196.
[25] S. H. Lim, A. G. Caster, S. R. Leone, *Opt. Lett.* **2007**, *32*, 1332.
[26] E. M. Vartiainen, H. A. Rinia, M. Müller, M. Bonn, *Opt. Express* **2006**, *14*, 3622.
[27] Y. Liu, Y. J. Lee, M. T. Cicerone, *Opt. Lett.* **2009**, *34*, 1363.
[28] W. L. Meerts, M. Schmitt, *Int. Rev. Phys. Chem.* **2006**, *25*, 353.
[29] M. H. Hennessy, A. M. Kelley, *Phys. Chem. Chem. Phys.* **2004**, *6*, 1085.
[30] N. Hansen, The CMA evolution strategy: a tutorial, **2010**, http://www.lri.fr/~hansen/cmatutorial.pdf.
[31] R. Fanciulli, L. Willmes, J. Savolainen, P. van der Walle, T. Bäck, J. L. Herek, *Lect. Notes Comput. Sci.* **2008**, *4926*, 219.
[32] A. C. W. van Rhijn, H. L. Offerhaus, P. van der Walle, J. L. Herek, A. Jafarpour, *Opt. Express* **2010**, *18*, 2695.